Relating mass and number to geometric mean diameter

Geometric mean diameter is related to mass and number through the following equations from table S1 in Liu et al., 2012:

$$D_g = \frac{D_{emit}}{\exp\left(\frac{3}{2}(\ln(\sigma_g))^2\right)}, \text{ Eq. S1}$$

Here, D_{emit}, or volume mean diameter, is defined by aerosol mass (E_{mass}) and number (E_{number})

$$D_{emit} = \left(\frac{E_{mass}}{\frac{\pi}{6}\rho E_{number}}\right)^{\frac{1}{3}}, \text{ Eq. S2}$$

Table S1: The different volcanic aerosol mode characteristics as well as the coarse mode dust and seasalt tuning factors used in the prognostic stratospheric aerosol models.

Model Version	**MAM4 aerosol size properties**	**Dust and seasalt emission tuning factors**
E3SMv2-PA	• Accumulation ○ $D_{gn,high}$: 0.44 µm ○ σ_g: 1.8 • Coarse ○ $D_{gn,high}$: 4.0 µm ○ $D_{gn,low}$: 1.0 µm ○ σ_g: 2.0	• dust_emis_factor = 1.5 • seasalt_emis_scale = 0.6
E3SMv2-SPA	• Accumulation ○ $D_{gn,high}$: 0.48 µm ○ σ_g: 1.6 • Coarse ○ $D_{gn,high}$: 40 µm ○ $D_{gn,low}$: 0.4 µm ○ σ_g: 1.2	• dust_emis_factor = 3.255 • seasalt_emis_scale = 0.36
CESM2-WACCM	• Accumulation ○ $D_{gn,high}$: 0.48 µm ○ σ_g: 1.6 • Coarse ○ $D_{gn,high}$: 40 µm ○ $D_{gn,low}$: 0.4 µm ○ σ_g: 1.2	• dust_emis_factor = 0.7 • seasalt_emis_scale = 0.9

Table S2: Aerosol properties from the 18 km WOPC and model comparison in Fig. 5. In this table, we diverge from the MAM4 naming convention of accumulation mode as the first mode, Aitken as the second mode, and coarse as the third mode – instead, we number them by increasing size. For the WOPC data, modes 1 and 2 are assumed to be accumulation and coarse, and for the models modes 1, 2, and 3 an are Aitken, accumulation, and coarse, respectively.

Date	**Source**	**Effective Radius**	**Mode**	**Dg**	**n(Dg)**	**Sigma**
19910419	WOPC	0.344±0.17	1	0.145±0.015	11.4±1.1	1.49
			2	0.918±0.09	0.7±0.07	1.05
	E3SMv2-PA	0.339	1	0.055	3.25	1.6
			2	0.145	3.93	1.8
			3	1.0	1.5×10^{-9}	2.0
	E3SMv2-SPA	0.318	1	0.052	2.25	1.6
			2	0.181	5.48	1.6
			3	0.711	0.02	1.2
	CESM2-WACCM		1	0.042	8.01	1.6
			2	0.172	7.39	1.6
			3	0.738	0.15	1.2
19910716	WOPC	0.332±0.09	1	0.077±0.008	9.8±1.0	2.14
	E3SMv2-PA	0.356	1	0.041	12.02	1.6
			2	0.154	5.08	1.8
			3	1.0	2.0×10^{-9}	2.0
	E3SMv2-SPA	0.328	1	0.037	11.1	1.6
			2	0.19	6.9	1.6
			3	0.79	0.03	1.2
	CESM2-WACCM		1	0.034	376.5	1.6
			2	0.163	22.0	1.6
			3	0.855	0.14	1.2
19911230	WOPC	0.882±0.31	1	0.361±0.04	18.2±1.8	1.27
			2	0.954±0.1	5.2±0.5	1.28
	E3SMv2-PA	0.992	1	0.052	0.02	1.6
			2	0.415	14.0	1.8
			3	1.1	1.2×10^{-9}	2.0
	E3SMv2-SPA	0.731	1	0.052	0.29	1.6
			2	0.271	17.8	1.6
			3	0.819	12.0	1.2
	CESM2-WACCM		1	0.059	0.25	1.6
			2	0.325	20.7	1.6
			3	0.909	21.5	1.2

19920508	WOPC	1.24±0.39	1	0.909±0.09	15.3±1.5	1.23
			2	1.92±0.19	2.8±0.3	1.09
	E3SMv2-PA	0.753	1	0.052	0.03	1.6
			2	0.316	9.5	1.8
			3	1.31	5.46×10^{-10}	2.0
	E3SMv2-SPA	0.8	1	0.052	0.09	1.6
			2	0.334	14.1	1.6
			3	0.828	19.76	1.2
	CESM2-WACCM		1	0.052	0.41	1.6
			2	0.352	13.48	1.6
			3	0.918	16.24	1.2
19920717	WOPC	1.12±0.53	1	0.46±0.05	11.9±1.2	1.35
			2	1.41±0.14	3.9±0.4	1.18
	E3SMv2-PA	0.71	1	0.052	0.26	1.6
			2	0.298	7.75	1.8
			3	1.21	7.1×10^{-10}	2.0
	E3SMv2-SPA	0.8	1	0.052	0.4	1.6
			2	0.343	11.8	1.6
			3	0.828	15.5	1.2
	CESM2-WACCM		1	0.041	1.29	1.6
			2	0.325	12.5	1.6
			3	0.936	10.9	1.2
19921218	WOPC	0.966±0.47	1	0.298±0.03	8.95±0.9	1.38
			2	0.99±0.1	6.3±0.6	1.23
	E3SMv2-PA	0.509	1	0.052	0.41	1.6
			2	0.217	6.09	1.8
			3	1.0	1.04×10^{-8}	2.0
	E3SMv2-SPA	0.761	1	0.052	0.15	1.6
			2	0.334	10.28	1.6
			3	0.79	12.1	1.2
	CESM2-WACCM		1	0.057	0.36	1.6
			2	0.343	9.7	1.6
			3	0.882	9.74	1.2
19930408	WOPC	0.808±0.39	1	0.684±0.07	15.1±1.5	1.28
			2	1.82±0.18	0.22±0.02	1.03
	E3SMv2-PA	0.441	1	0.057	0.84	1.6
			2	0.189	5.61	1.8
			3	1.1	7.83×10^{-10}	2.0

	E3SMv2-SPA	0.705	1	0.052	0.27	1.6
			2	0.298	8.96	1.6
			3	0.765	7.77	1.2
	CESM2-WACCM		1	0.048	1.82	1.6
			2	0.298	9.31	1.6
			3	0.873	5.77	1.2
19930621	WOPC	0.866±0.39	1	0.244±0.02	13.8±1.4	1.47
			2	1.1±0.11	2.2±0.2	1.22
	E3SMv2-PA	0.467	1	0.05	3.99	1.6
			2	0.199	5.83	1.8
			3	1.0	1.9×10^{-9}	2.0
	E3SMv2-SPA	0.687	1	0.05	1.68	1.6
			2	0.289	8.77	1.6
			3	0.774	5.4	1.2
	CESM2-WACCM		1	0.037	6.5	1.6
			2	0.253	10.9	1.6
			3	0.927	3.23	1.2
19931116	WOPC	0.757±0.37	1	0.334±0.03	6.48±0.6	1.42
			2	0.95±0.1	1.95±0.2	1.2
	E3SMv2-PA	0.361	1	0.057	1.15	1.6
			2	0.154	4.43	1.8
			3	1.92	1.0×10^{-10}	2.0
	E3SMv2-SPA	0.62	1	0.052	0.24	1.6
			2	0.262	6.66	1.6
			3	0.711	3.71	1.2
	CESM2-WACCM		1	0.052	1.18	1.6
			2	0.262	7.12	1.6
			3	0.81	3.03	1.2

Table S3: Comparison of absorption efficiency at 10 μm from CESM2-WACCM model simulations given different complex refractive index assumptions. The complex refractive index n_{Hess} is akin to assuming no aerosol water (i.e., pure sulfate), while n_s includes the volume weighted contributions from n_{Hess} and n_{wat}.

Date	**Region**	Q_a (n_{Hess}, w/o water)	Q_a (n_s, volume-weighted water and sulfate)	% Difference
1991-04	41˚N	0.064	0.057	-12.3
	20˚S–20˚N	0.088	0.077	-14.3
1991-07	41˚N	0.094	0.084	-11.9
	20˚S–20˚N	0.104	0.092	-13.0
1991-12	41˚N	0.16	0.135	-18.5
	20˚S–20˚N	0.176	0.154	-14.3
1992-04	41˚N	0.165	0.139	-18.7
	20˚S–20˚N	0.178	0.156	-14.1
1992-07	41˚N	0.162	0.137	-18.3
	20˚S–20˚N	0.175	0.154	-13.6
1992-12	41˚N	0.154	0.129	-19.4
	20˚S–20˚N	0.167	0.146	-14.4
1993-04	41˚N	0.139	0.118	-17.8
	20˚S–20˚N	0.16	0.139	-15.1
1993-07	41˚N	0.129	0.11	-17.3
	20˚S–20˚N	0.15	0.131	-14.5
1993-12	41˚N	0.122	0.105	-16.2
	20˚S–20˚N	0.153	0.13	-17.7

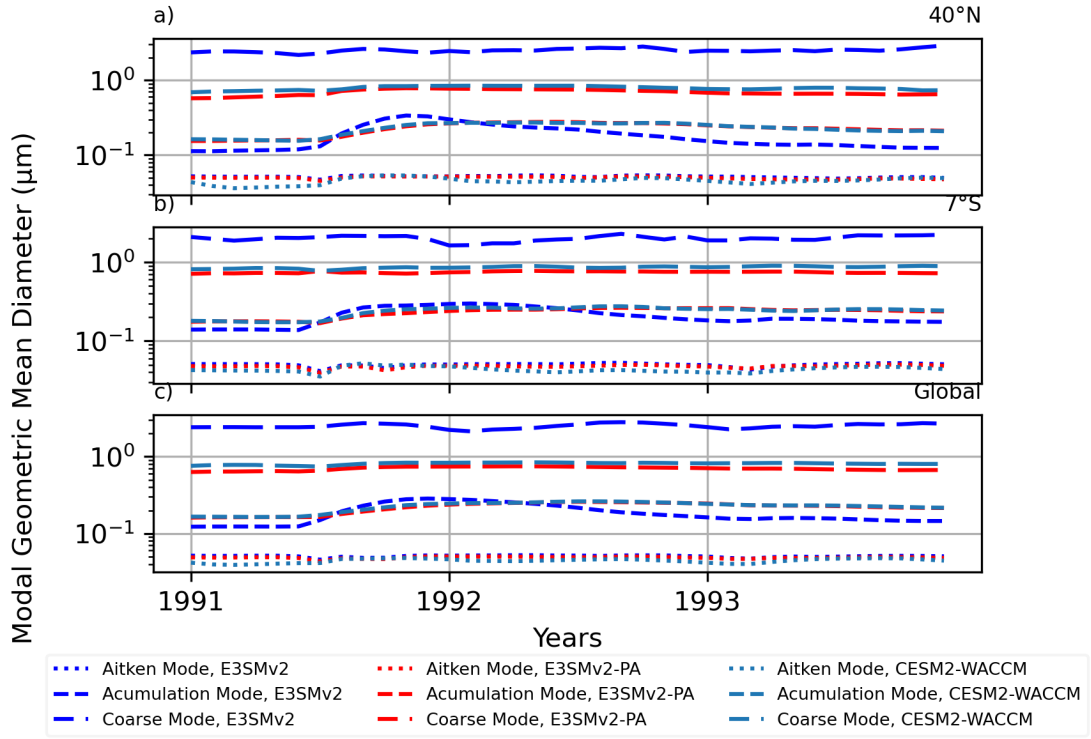

.

Figure S1: Modal aerosol diameters (μm) for the UARS regions (40˚N and 7˚S latitude bands; <=100 hPa) and globally averaged (<=100 hPa). Geometric mean diameters reported for Aitken (dotted), accumulation (dashed), and coarse modes (long dash).

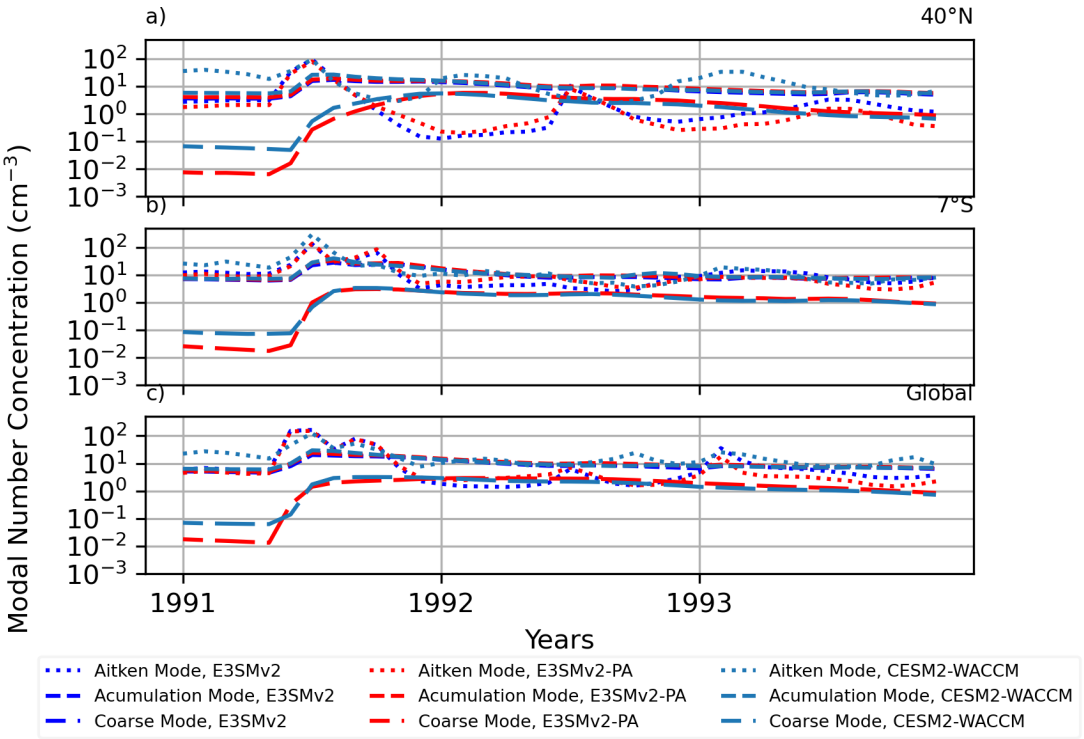

Figure S2: Modal aerosol number concentrations (cm^{-3}) for the UARS regions (40˚N and 7˚S latitude bands; <=100 hPa) and globally averaged (<=100 hPa). Geometric mean diameters reported for Aitken (dotted), accumulation (dashed), and coarse modes (long dash).

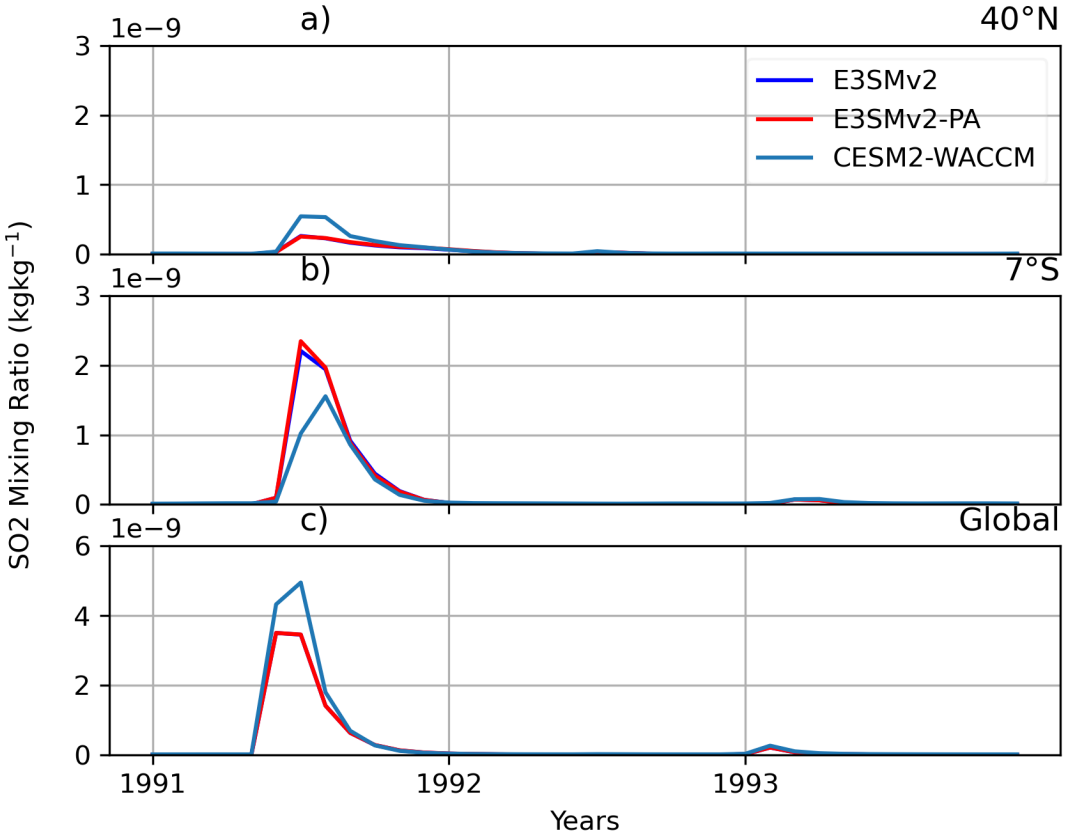

Figure S3: Sulfur dioxide mass mixing ratio (kg kg^{-1}) for the UARS regions (40˚N and 7˚S latitude bands; <=100 hPa) and globally averaged (<=100 hPa).

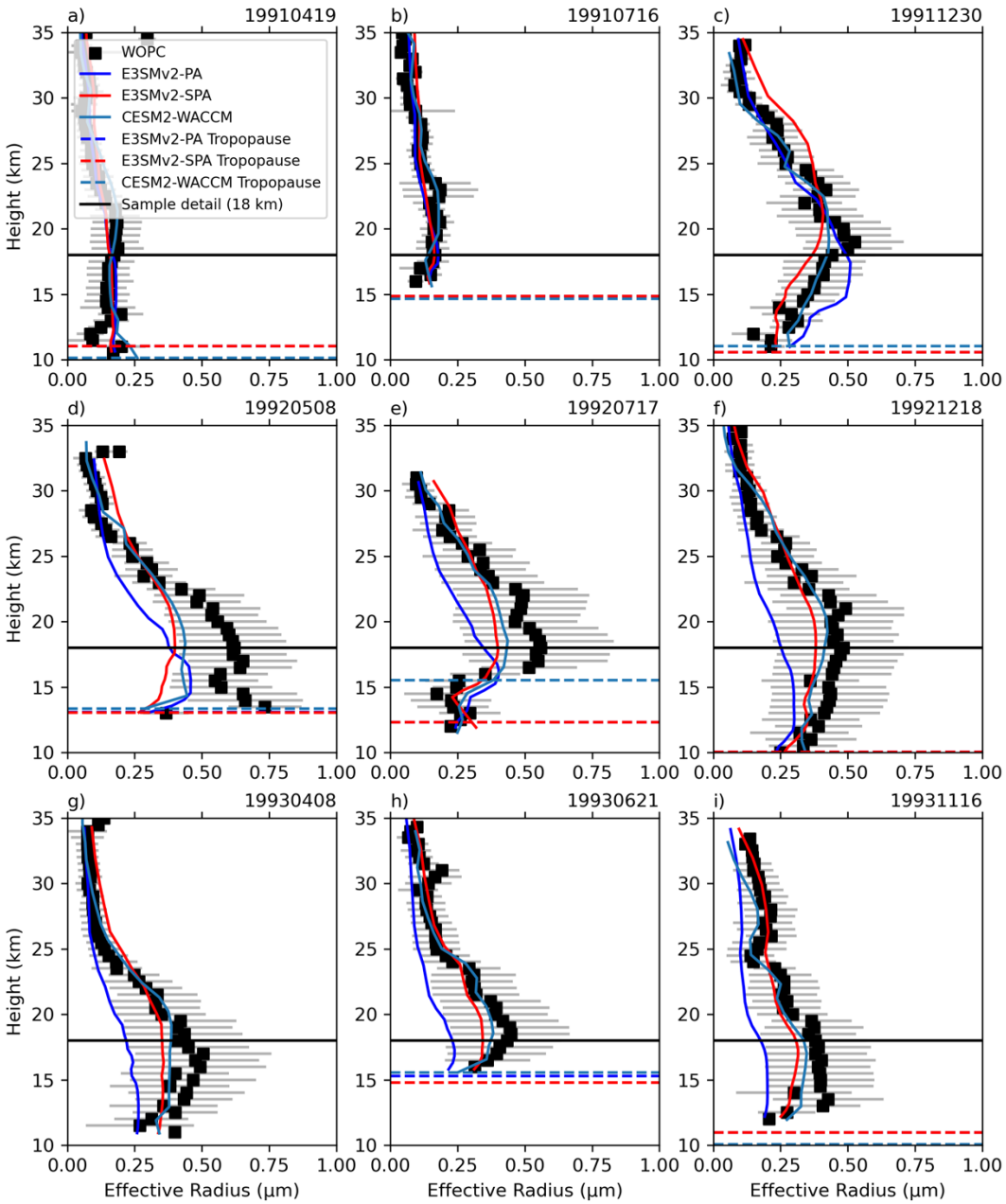

Figure S4: Vertical profiles of daily WOPC samples over Laramie (41ℕ 105℠W) compared to E3SM and CESM2-WACCM. Dashed lines show the model tropopause and the solid black line marks the 18 km sample level corresponding to size distributions in Fig. 5. Results are for a single grid cell.

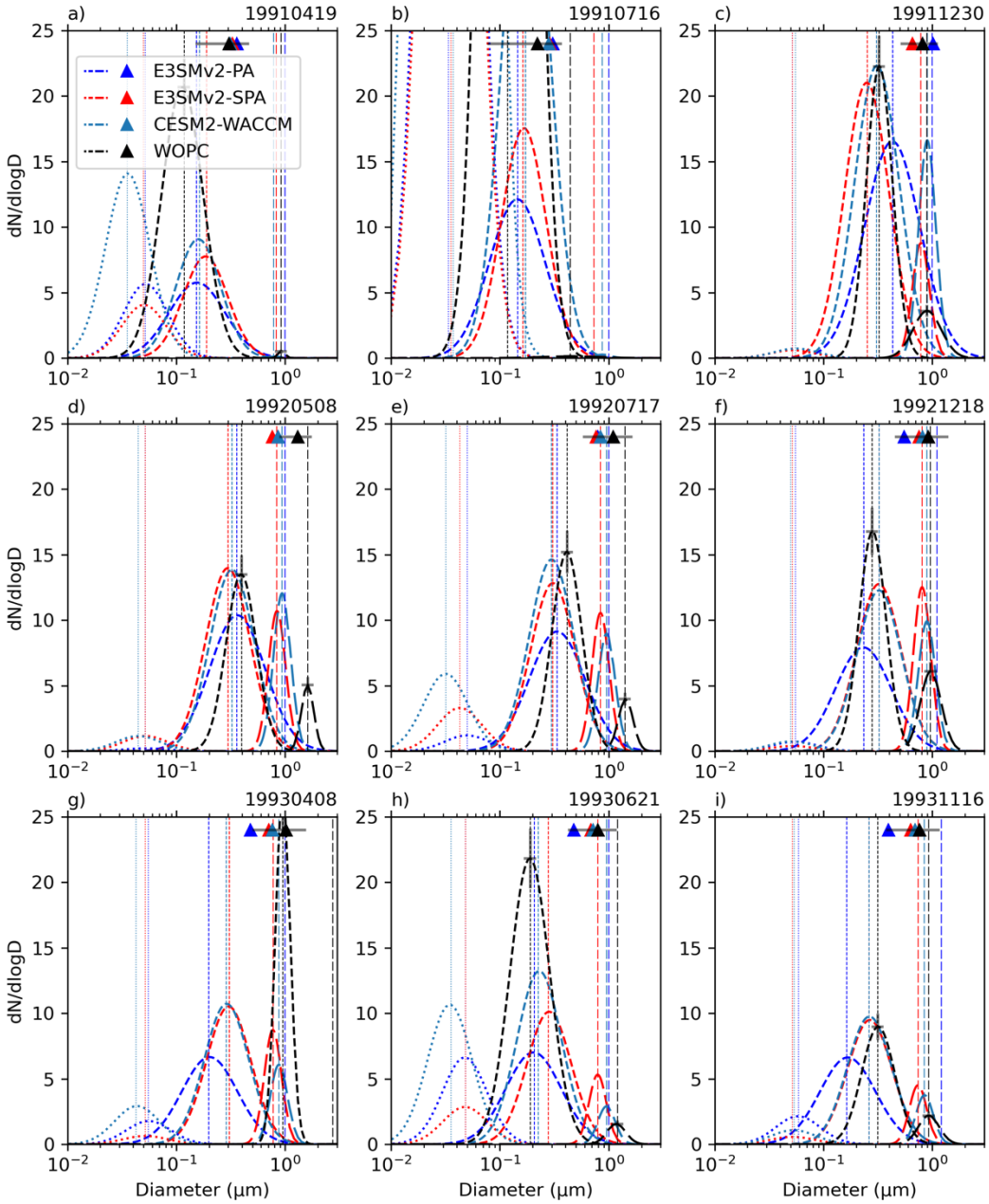

Figure S5: Same as Fig. 5, but for a 17 km sample level.

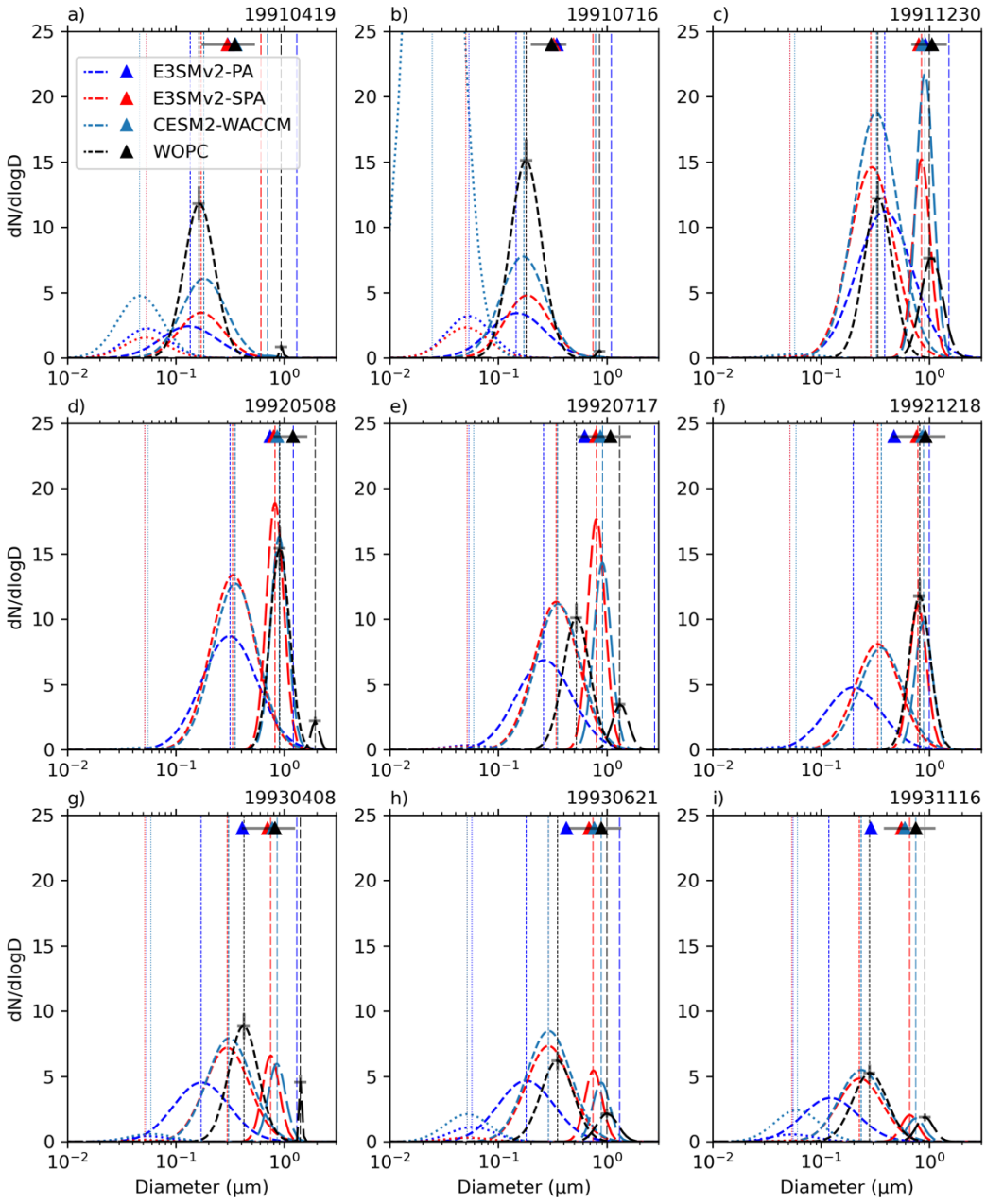

Figure S6: Same as Fig. 5, but for a 19 km sample level.

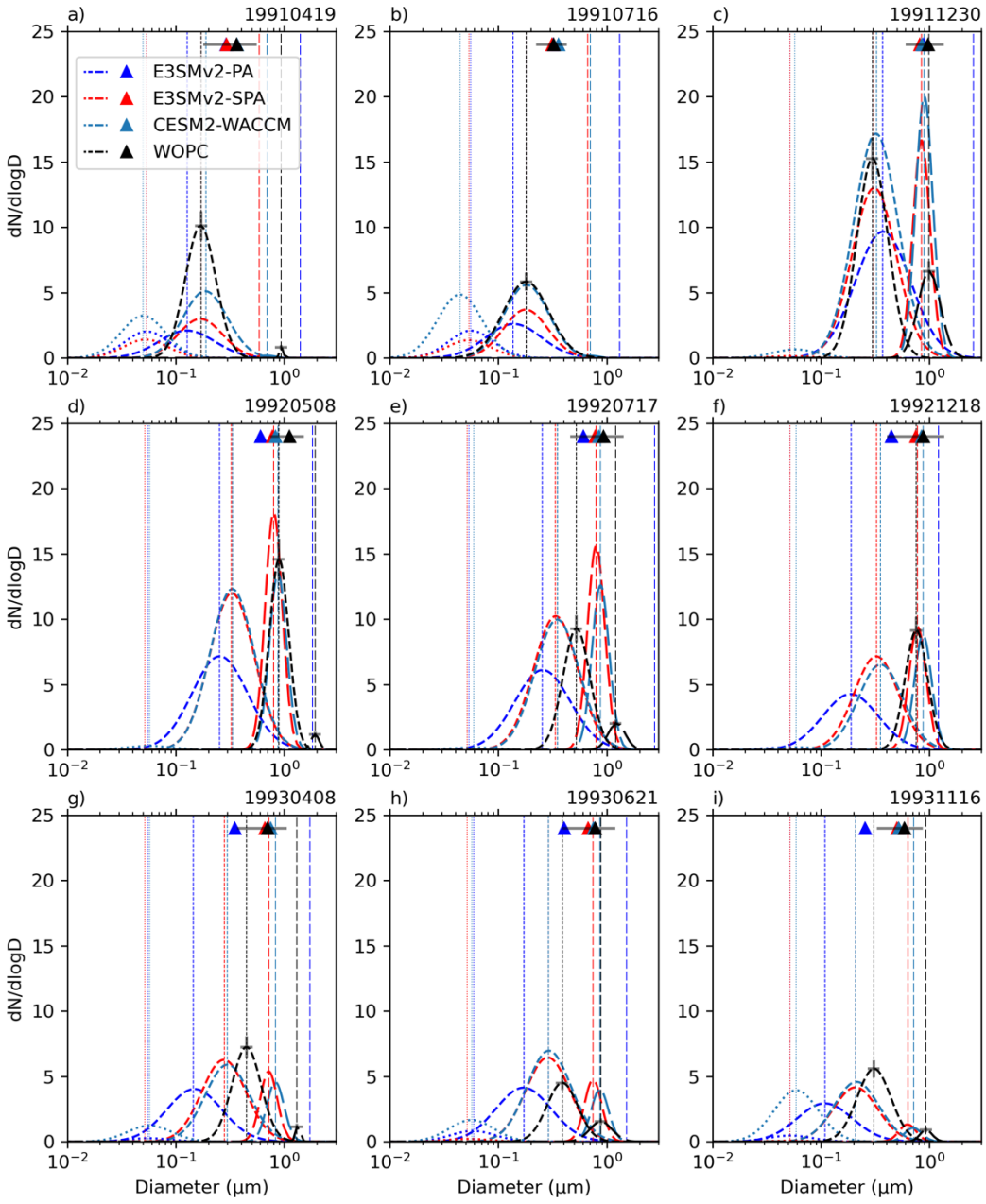

Figure S7: Same as Fig. 5, but for a 20 km sample level.

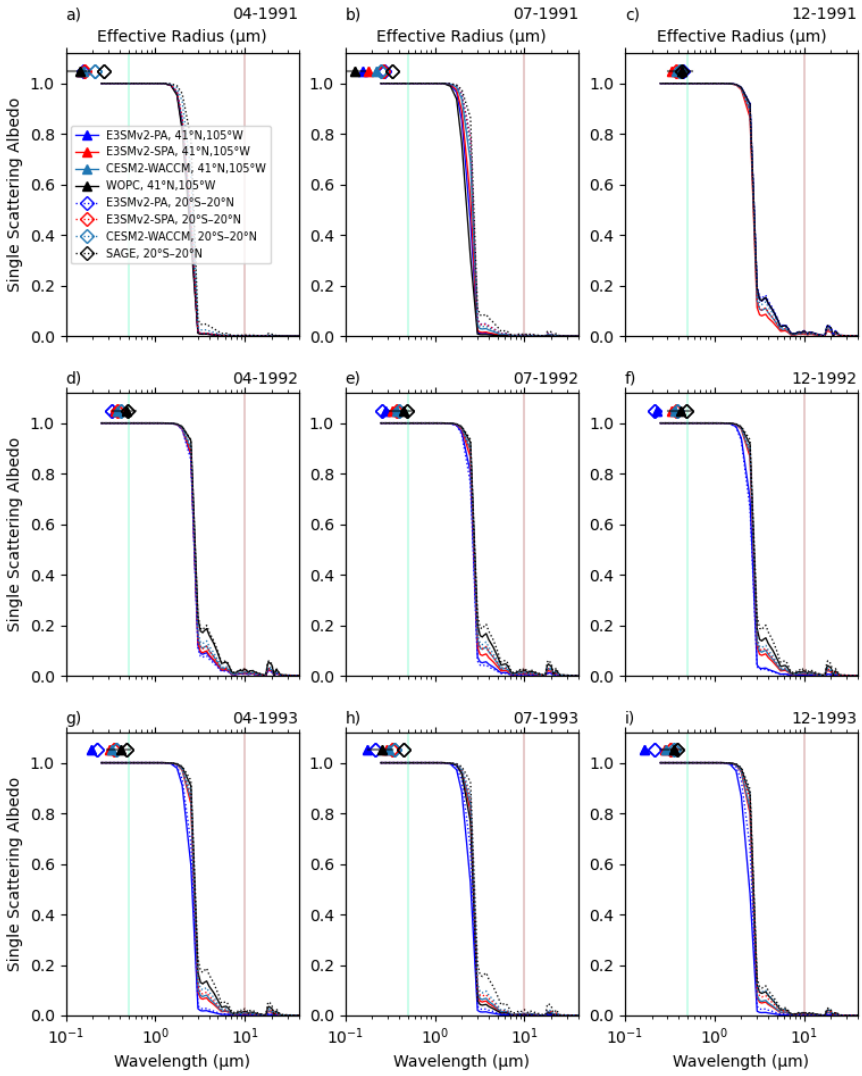

Figure S8: Single scattering albedo (SSA) calculated from effective radii and Hess et al. 0% RH sulfate refractive index. SSA is the ratio of the scattering and extinction efficiencies (Q_s/Q_e). Same sample regions as Figure 7: WOPC (41˚N 105˚W; 130-10 hPa) and SAGE (20˚S-20˚N; 50-10 hPa). The turquoise vertical line marks the solar black body wavelength of maximum irradiance (0.5 μm) and the dark red line marks the terrestrial black body wavelength of maximum irradiance (10 μm).

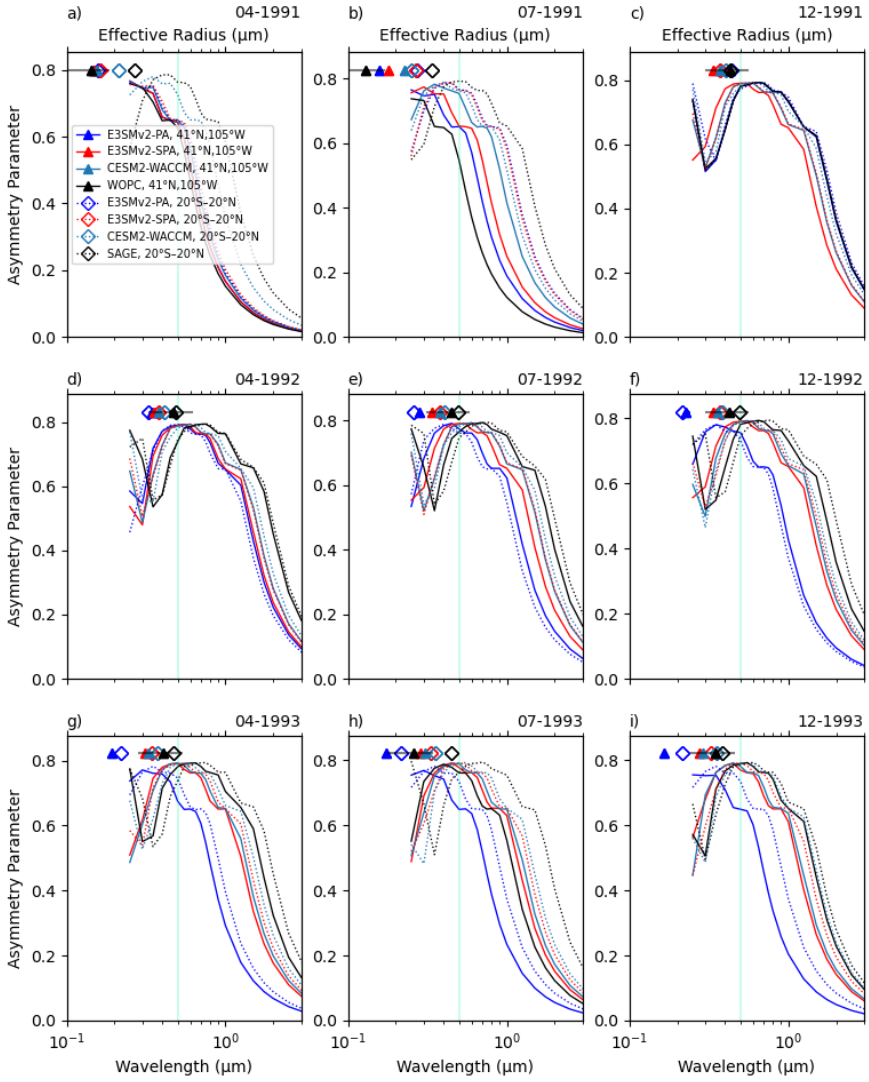

Figure S9: Asymmetry parameter (g) calculated from effective radii and Hess et al. 0% RH sulfate refractive index. The g is the intensity-weighted cosine of the scattering angle and ranges from 1 – -1, where g=1 is forward scattering, g=0 is isotropic scattering, and g=-1 is back scattering. Same sample regions as Figure 7: WOPC (41˚N 105˚W; 130-10 hPa) and SAGE (20˚S-20˚N; 50-10 hPa). The turquoise vertical line marks the solar black body wavelength of maximum irradiance (0.5 μm) and the dark red line marks the terrestrial black body wavelength of maximum irradiance (10 μm).

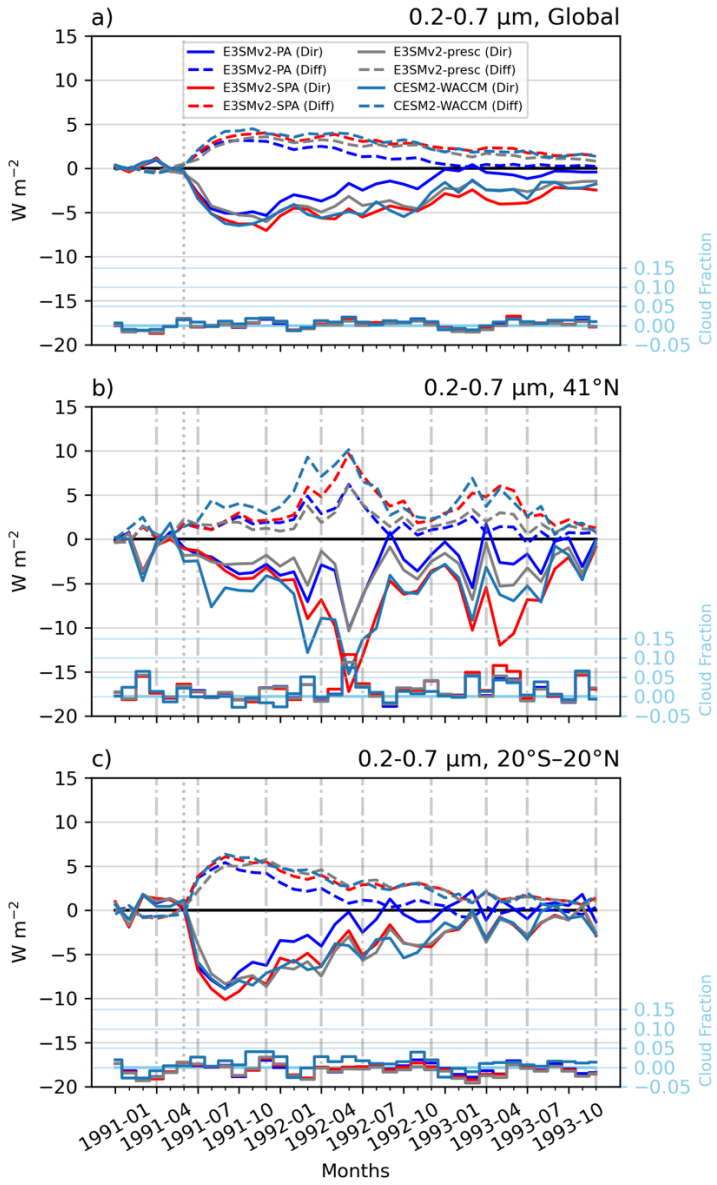

Figure S10: Same as Fig. 8 but for 0.7-5 µm wavelengths.

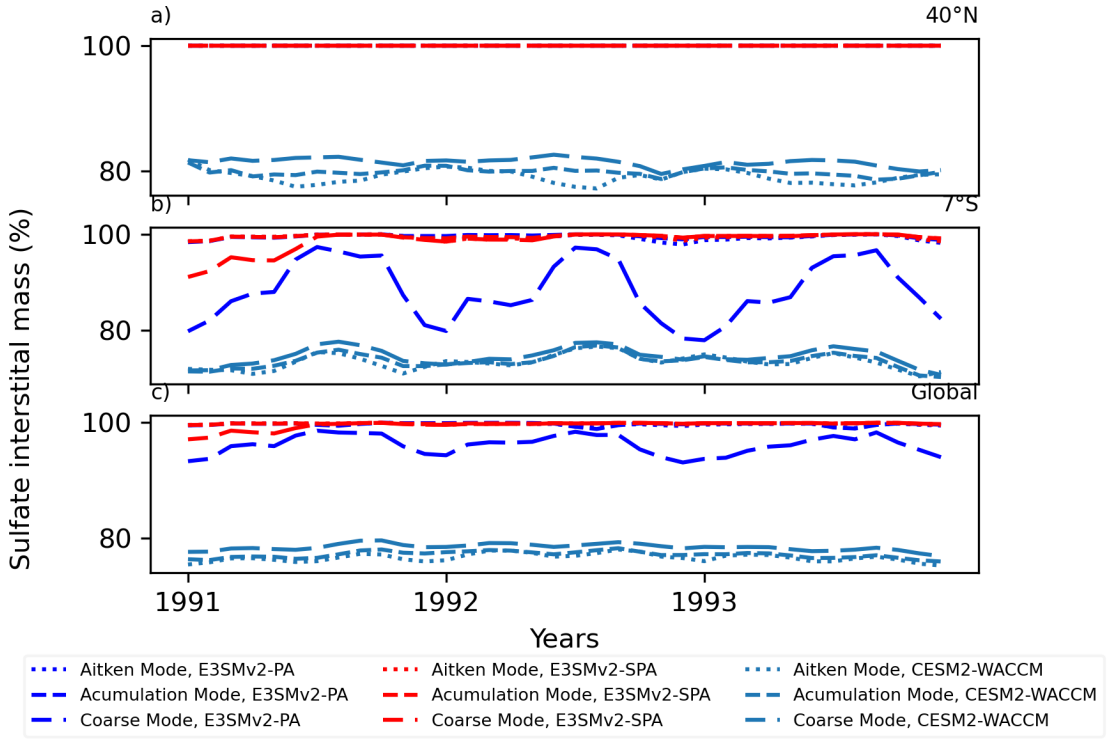

Figure S11: Percent of total mass (interstitial sulfate + interstitial water) composed of sulfate in the stratosphere for 40˚N, 7˚S, and global averages.